The stability of steady, helical vortex filaments in a tube

L. G. Sarasúa, A. C. Sicardi Schifino, and R. González

Citation: Physics of Fluids **11**, 1096 (1999); doi: 10.1063/1.869980
View online: https://doi.org/10.1063/1.869980
View Table of Contents: http://aip.scitation.org/toc/phf/11/5
Published by the American Institute of Physics

The stability of steady, helical vortex filaments in a tube

L. G. Sarasúa
Facultad de Ciencias, Universidad de la República, Montevideo, Uruguay

A. C. Sicardi Schifino
Facultad de Ciencias and Facultad de Ingeniería, Universidad de la República, Montevideo, Uruguay

R. González
Facultad de Ciencias Exactas y Naturales, Universidad de Buenos Aires, Buenos Aires, Argentina

(Received 22 September 1997; accepted 30 December 1998)

The nonlinear conditions for the development of helical vortex filaments in a circular tube are considered. The helical flow is assumed to be irrotational, except in a vortex filament of infinitesimal core area. By introducing an appropriate image for this helical vortex filament, the boundary condition on the material frontier is satisfied. By assuming an axisymmetric flow upstream and imposing the conservation laws, a dependence between the helix pitch and the nonlinear amplitude of the helical vortex developed downstream is obtained. Our results show that only helical flows with the pitch in a certain range of values are allowed. The dependence of this range on the swirl ratio and on the tube cross section is considered. We discuss the usefulness of the nonlinear analysis of the allowed flows to explain experimental results and to complement the usual linear study of stability. © *1999 American Institute of Physics.* [S1070-6631(99)01904-2]

I. INTRODUCTION

In recent years, there has been an important number of theoretical and experimental results on the development of structural changes in vortex flows. These phenomena, which produce abrupt unsteady changes in the pressure of the fluid, are usually associated with a loss of axial symmetry. They are of interest in several technical applications (for example, in aerodynamics and in the design of hydraulic machineries, as hydroelectric turbines). Laboratory experiments in tubes, described in Refs. 1–3, show that the flow is essentially irrotational, with constant circulation, except in a helical rotational core. (When the phenomenon just appears, the rotational core is close to the tube axis.)

In this work, we study the possible steady, helical vortex filaments with finite helix radius (i.e., with arbitrary departure from an axially symmetric flow). To investigate the mechanisms that govern the structural changes in the flow, we consider the initial (inflow) field as axially symmetric and confined to a tube. We assume that (everywhere along the tube) the flow is irrotational except in a rotational core filament, with infinitesimal area and constant circulation around it. In Sec. II, the basic equations are derived. In Sec. III, an expression for the velocity field of the helical vortex filament is obtained, taking into account the material boundary conditions. In Sec. IV, a given upstream flow is considered and, by imposing conservations laws, a rule is obtained for the possible helical vortex filaments which can develop downstream departing from the axially symmetric flow. In Sec. V, criteria for the vortex stability are considered. In Sec. VI, the results of our analysis are applied to concrete examples.

II. BASIC EQUATIONS

We assume that the flow is incompressible and irrotational everywhere except in a vortex filament, i.e., in an infinite concentrated rotational core.

In the case of an incompressible inviscid fluid, the governing equations are $\nabla.\mathbf{v}=0$ and the Euler equation. In terms of the vorticity $\mathbf{w}=\nabla\times\mathbf{v}$, the Euler equation takes the form of an evolution equation

$$\frac{\partial \mathbf{w}}{\partial t}+\mathbf{v}\cdot\nabla\mathbf{w}=\mathbf{w}\cdot\nabla\mathbf{v}. \tag{1}$$

Therefore, the circulation

$$\Gamma=\oint_C \mathbf{v}\cdot d\mathbf{l} \tag{2}$$

is governed by the Kelvin theorem $((\partial/\partial t)+\mathbf{v}\cdot\nabla)\Gamma=0$. That is to say, the vortex filament moves with constant circulation around it.

When the vorticity is concentrated, in the unbounded flow case, the velocity is determined by the Biot–Savart law;

$$\mathbf{v}_u(\mathbf{r})=\frac{\Gamma}{4\pi}\int_l \frac{(\mathbf{r}-\mathbf{r}')\times d\mathbf{l}'}{|\mathbf{r}-\mathbf{r}'|^3}. \tag{3}$$

However, if boundary walls are present, this expression is not valid, because (in general) it does not satisfy the boundary conditions. We can construct an adequate solution for the flow around the vortex filament, adding to Eq. (3) a field $\mathbf{v}_b(\mathbf{r})$, with $\nabla\times\mathbf{v}_b=0$ and $\nabla\cdot\mathbf{v}_b=0$, provided that the sum

$$\mathbf{v}(\mathbf{r})=\frac{\Gamma}{4\pi}\int_l \frac{(\mathbf{r}-\mathbf{r}')\times d\mathbf{l}'}{|\mathbf{r}-\mathbf{r}'|^3}+\mathbf{v}_b(\mathbf{r}) \tag{4}$$

satisfies the condition

$$\mathbf{n}\cdot\mathbf{v}|_s=\mathbf{n}\cdot(\mathbf{v}_u+\mathbf{v}_b)|_s=0 \tag{5}$$

on the limiting surface, where $\mathbf{n}$ is the unit vector in the normal direction to the surface. We note that $\mathbf{v}_b$ depends on $\mathbf{v}_u$ in a nonlinear form.

Using Eq. (1) it is possible to prove (see Batchelor[4]) that the vortex filament core moves with the particles without changes in the core strength (vorticity-transport theorem). That is to say, the vortex line displacement $\delta\mathbf{l}$ is

$$\delta\mathbf{l}=\mathbf{v}|_{r=r_c}\delta t, \tag{6}$$

where r_c is the position of the vortex line.

In principle, by using the previous equations, we could determine the vortex motion. However, this presents a serious difficulty in practice, because the first term of Eq. (4) is divergent when it is calculated on the filament itself (Batchelor[4]). Obviously this singularity is unphysical because the real vortex has a finite core where Eq. (4) is not valid. Thus to determine the vortex velocity at the core, the real finite vortex core properties[5–8] must be considered. As a consequence, the resulting vortex motion depends critically on the core characteristics, and so the method is not very useful when the core size is not precisely known. In our work, we use only globally conserved magnitudes (as the mass rate, the circulation, and the total angular momentum), which do not depend on the vortex core characteristics. As we show in Sec. IV, significant results can be obtained which are independent of the concrete value of the core size, provided it is small in relation with the tube radius.

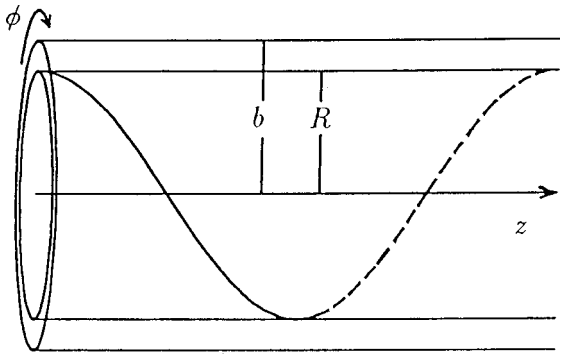

FIG. 1. The coordinate system and the helical vortex filament.

III. HELICAL VORTEX FILAMENTS IN A TUBE

In this work, we restrict our attention to the steady helical flows allowed inside a tube of radius b which can be modeled as vortex filaments. We assume that the helical vortex line has constant circulation along its extension and is situated on a cylinder of radius $R<b$, with pitch λ (see Fig. 1). As there are two possible geometrical senses for the helix, we consider that λ can be positive or negative so that the sign of λ determines the sense of the helix. The filament can be parameterized as a line with an angular parameter α,

$$x=R\sin\alpha,\quad y=R\cos\alpha,\quad z=\lambda\alpha/2\pi, \tag{7}$$

where α varies between $-\infty$ and $+\infty$.

The helical flow depends only on the helical coordinates (r,ϕ), where $\phi=\theta-(2\pi/\lambda)z$ and (r,θ,z) are the usual cylindrical coordinates. From Eqs. (3) and (7), we obtain the following expression for $\mathbf{v}_u$:

$$v_{ux}=F_x(r,\phi,R,\lambda,\Gamma)=\frac{\Gamma}{4\pi}\int_{-\infty}^{\infty}\frac{\left(-R\sin\alpha\left(z-\frac{\lambda}{2\pi}\right)-\frac{\lambda}{2\pi}(r\sin\phi-R\cos\alpha)\right)d\alpha}{\sqrt{((r\cos\phi-R\sin\alpha)^2+(r\sin\phi-R\cos\alpha)^2+(z-\lambda\alpha/2\pi)^2)^3}},$$

$$v_{uy}=F_y(r,\phi,R,\lambda,\Gamma)=\frac{\Gamma}{4\pi}\int_{-\infty}^{\infty}\frac{\left(\frac{\lambda}{2\pi}(r\cos\phi-R\sin\alpha)-R\cos\alpha\left(z-\frac{\lambda}{2\pi}\right)\right)d\alpha}{\sqrt{((r\cos\phi-R\sin\alpha)^2+(r\sin\phi-R\cos\alpha)^2+(z-\lambda\alpha/2\pi)^2)^3}},$$

$$v_{uz}=F_z(r,\phi,R,\lambda,\Gamma)=\frac{\Gamma}{4\pi}\int_{-\infty}^{\infty}\frac{(Rr\sin\phi\cos\alpha+Rr\cos\phi\sin\alpha-R^2)d\alpha}{\sqrt{((r\cos\phi-R\sin\alpha)^2+(r\sin\phi-R\cos\alpha)^2+(z-\lambda\alpha/2\pi)^2)^3}}. \tag{8}$$

We construct the function $\mathbf{v}_b$, considering it as the velocity field of an induced image vortex, characterized by a radius $R^*>b$, a circulation Γ^*, and the same pitch λ. In this case, the total velocity field is

$$\mathbf{v}=\mathbf{F}(r,\phi,R,\lambda,\Gamma)+\mathbf{F}(r,\phi,R^*,\lambda,\Gamma^*)+U_0\mathbf{e}_z,$$

$$\equiv\mathbf{v}_h(r,\phi,R,\lambda,\Gamma)+U_0\mathbf{e}_z, \tag{9}$$

where $U_0\mathbf{e}_z$ is an arbitrary constant term.

In the case of straight vortices ($\lambda\to\infty$), the values of R^* and Γ^* can be computed using the well known Milne–Thompson theorem.[9] This theorem states that $\Gamma^*=-\Gamma$ and $R^*=b^2/R$. Unfortunately, there does not exist a general result for the case with finite λ. In this work, numerical values of R^* and Γ^* (for given Γ, R, and λ) are determined by imposing condition (5) on some selected points on the surface, as shown in Fig. 2. In points 1 and 4 this condition holds automatically. We determine R^* and Γ^* by imposing condition (5) in points 2 and 3 (and solving the system of the two resulting equations). Then, because of the symmetry, it is also satisfied in the points 5 and 6. Therefore, condition (5) holds exactly in the points (P_i, $i=1,6$) on the surface (see Fig. 2). It also holds approximately in other points around

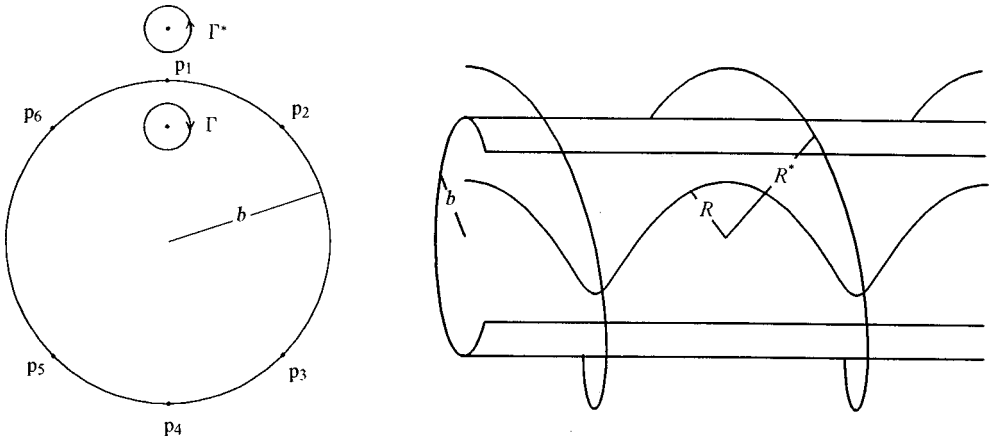

FIG. 2. Sketch of the helical vortex filament and the image vortex showing the points on the surface where is imposed the tangency boundary condition (5).

the surface (we verified this numerically). It is important to note that we need to evaluate the velocity field only on some points at the wall. Then, the divergence at the core does not affect our calculation. Thus we do not require to use special techniques of desingularization to solve the system. (In doing so, we eliminate Γ^* and then use a numerical bisection method to solve the resulting equation for R^*, evaluating the integrals for each value of R^*.)

In Fig. 3, the curves denote the values of Γ^* and R^* in the function of R and λ, taking $b=1$ and $\Gamma=1$. In this figure, it can be seen that as $\lambda\to\infty$, the numerical values for R^* and Γ^* approach those obtained from the Milne–Thompson theorem, as expected. As mentioned before, these values are calculated considering only a finite number of points on the limiting surface. However, on the material frontier surface, the normal component of the velocity, $\mathbf{n}\cdot\mathbf{v}|_s$, is always less than 0.5% of the parallel velocity component. Then, Eq. (9) represents a good approximation to the flow, for our purpose (see Fig. 4). So, using Eqs. (9), (8), and the results shown in Fig. 3, we can determine the helical vortex filament for arbitrary values of R and λ.

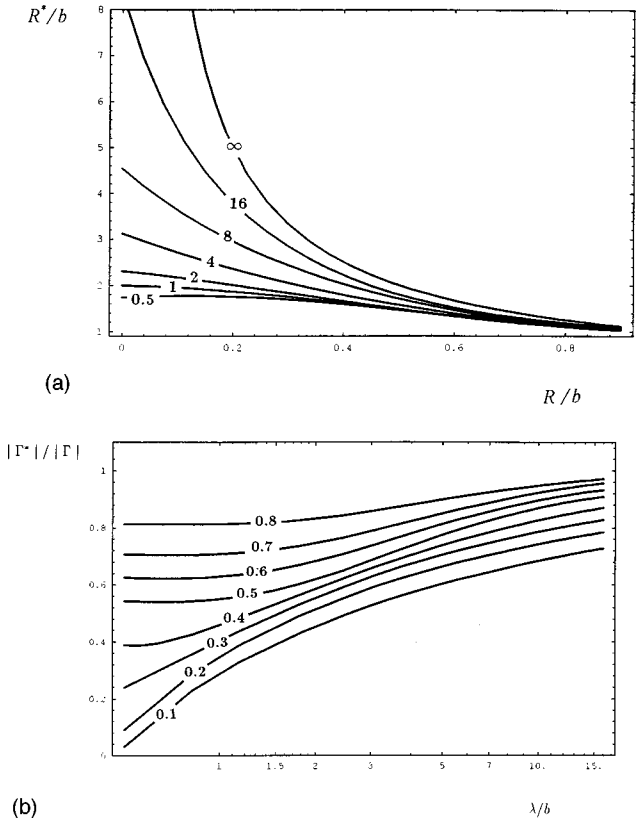

FIG. 3. (a) Distance from the axis to the helical image vortex R^* in function of R and the pitch λ of the helical vortex filament. (b) Absolute value of the ratio of the image vortex circulation Γ^* and the helical vortex circulation Γ, in function of R and λ.

IV. ADMISSIBLE FLOWS

In this section, we particularize the previous analysis (valid for arbitrary values of R, λ, and Γ) to the special case in which the flow comes from an upstream cylindrical region with radius b_1, where the velocity field is

$$v_{\theta 1}=\frac{\Gamma_0}{2\pi r},\quad v_{z1}=U_1,\quad v_{r1}=0. \tag{10}$$

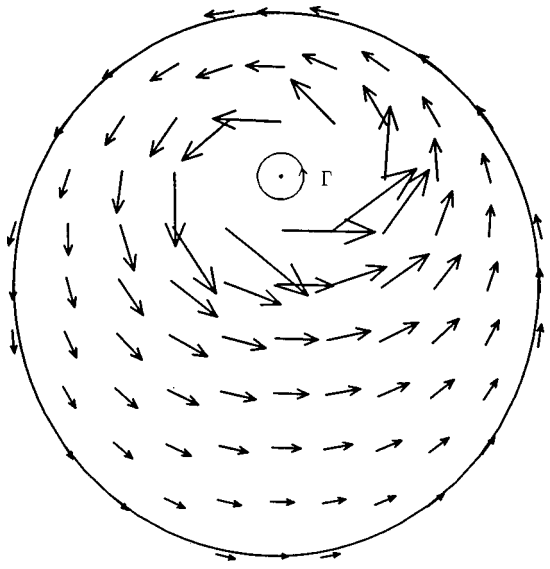

FIG. 4. Velocity field of the helical vortex filament for $R=0.4$, $\lambda=2$, and $b=1$.

The downstream region is also considered to be cylindrical, but with radius b_2. We suppose that the transition between the tubes is smooth enough to neglect transient effects. We are interested in determining the possible values of R and λ for the helical vortex filament developed in the downstream region. In order to determine these parameters, we impose the conservation of global magnitudes.

First, we note that the Kelvin theorem implies that the circulation must be the same in both the upstream and downstream regions, that is to say, $\Gamma=\Gamma_0$. On the other hand, if an helical flow is present, it must satisfy the mass and angular momentum conservation.

A. Mass flux of the helical vortex

If we assume that the cross section area of the core is very small, in relation to the tube cross section area, the flow rate at the core can be neglected. In order to calculate the mass flow rate of the helical vortex filament, it is useful to introduce the vector potential of the velocity field. The surface integral of the velocity along the cross surface can be computed using Stokes theorem, integrating the potential vector round a closed curve C situated on the tube surface. This procedure avoids the singularities at the core, as we have mentioned in Sec. II. The potential vector $\mathbf{H}(\mathbf{r})$ of the partial field (3) is easily obtained from the expression

$$\mathbf{H}(\mathbf{r})=\frac{\Gamma}{4\pi}\int_l \frac{d\mathbf{l}'}{|\mathbf{r}-\mathbf{r}'|}. \tag{11}$$

So, if we call

$$\begin{aligned} H_x(r,\phi,R,\lambda,\Gamma)&=\frac{\Gamma}{4\pi}\int_{-\infty}^{\infty}\frac{R\cos\alpha\, d\alpha}{\sqrt{((r\cos\phi-R\sin\alpha)^2+(r\sin\phi-R\cos\alpha)^2+(z-\lambda\alpha/2\pi)^2)}},\\ H_y(r,\phi,R,\lambda,\Gamma)&=\frac{\Gamma}{4\pi}\int_{-\infty}^{\infty}\frac{-R\sin\alpha\, d\alpha}{\sqrt{((r\cos\phi-R\sin\alpha)^2+(r\sin\phi-R\cos\alpha)^2+(z-\lambda\alpha/2\pi)^2)}}, \end{aligned} \tag{12}$$

the potential vector $\mathbf{A}$ of the total velocity field is

$$\begin{aligned} \mathbf{A}(r,\phi)&=\mathbf{H}(r,\phi,R,\lambda,\Gamma)+\mathbf{H}(r,\phi,R^*,\lambda,\Gamma^*)+\tfrac{1}{2}U_0 r\mathbf{e}_0,\\ &\equiv\mathbf{A}_h(r,\phi)+\tfrac{1}{2}U_0 r\mathbf{e}_\theta, \end{aligned} \tag{13}$$

Then the mass conservation leads to the constraint

$$\pi b_1^2 U_1=\pi b_2^2 U_0+\int_G \mathbf{A}_h(r,\phi)\cdot d\mathbf{l}. \tag{14}$$

Helical stream function

When an incompressible flow depends only on the helical coordinates (r,ϕ), it is possible to define a stream function $\Psi(r,\phi)$ such that

$$v_r=\frac{1}{r}\frac{\partial\Psi}{\partial\phi},\quad v_\phi=-\frac{\partial\Psi}{\partial r} \tag{15}$$

where $v_\phi=v_\theta-(2\pi/\lambda)v_z$. Taking derivatives, it can be seen that $\Psi=A_z+(2\pi/\lambda)A_\theta$, where A_z, A_θ are the components of the velocity vector potential. From this last equality and Eq. (13), we can also find immediately the expression for the helical flow stream function $\Psi(r,\phi)$.

B. Flux of angular momentum

Let us consider that the streamlines which form the surfaces S_1,S_2 in the upstream region, form corresponding surfaces S_1',S_2' in the downstream region. If there is a helical flow, the section of surfaces S_1',S_2' looks as it is shown in Fig. 5 (we take S_2 and S_2' on the material frontier). The mass conservation and the fluid incompressibility imply that the volume rate between surfaces S_1',S_2' is the same that between S_1,S_2. Furthermore, as a consequence of the axial symmetry of the duct, the flow does not experiment a net torque and it conserves its angular momentum in relation to the tube axis. These two conditions lead to the equalities

$$\begin{aligned} 2\pi b_1 h_1 v_{z1}&=\int_0^{2\pi} h_2(\phi)v_{z2}(\phi)b_2\, d\phi,\\ 2\pi b_1^2 h_1 v_{z1}v_{\theta 1}&=\int_0^{2\pi} h_2(\phi)v_{z2}(\phi)v_{\theta 2}(\phi)b_2^2\, d\phi, \end{aligned} \tag{16}$$

where $h_2(\phi)$ is the radial separation between S_1' and S_2'. By combining these equations, we obtain the condition

$$b_1 v_{\theta 1}=b_2\frac{\int_0^{2\pi}h_2(\phi)v_{z2}(\phi)v_{\theta 2}(\phi)d\phi}{\int_0^{2\pi}h_2(\phi)v_{z2}(\phi)d\phi}. \tag{17}$$

Now, we assume that the stream function value Ψ is constant on surfaces S_1',S_2' with corresponding values Ψ_1,Ψ_2. When h is small, we can write that $\Psi_2-\Psi_1\simeq h(\partial\Psi/\partial r)|_{r=b}$. Using Eq. (15), we obtain $h_2(\phi)\simeq(\Psi_1$

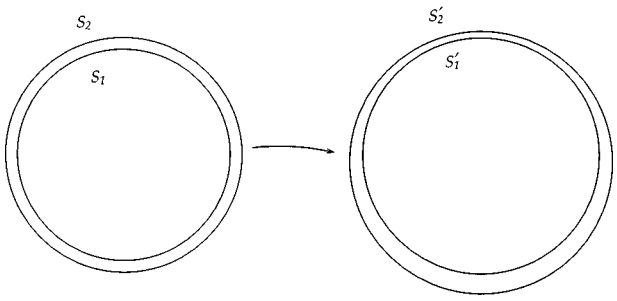

FIG. 5. Cross-section of the streamlines surfaces, upstream and downstream, when it is present downstream a helical flow.

$-\Psi_2)/v_\phi$, where $\Psi_1-\Psi_2$ is independent of ϕ. Substituting in Eq. (17) and making simplifications, we finally obtain the following constraint equation

$$b_1 v_{\theta 1} = b_2 \frac{\int_0^{2\pi} g(\phi) v_{\theta 2}(\phi) d\phi}{\int_0^{2\pi} g(\phi) d\phi} \equiv b_2 \langle v_{\theta 2} \rangle .$$

In order to calculate the average $\langle v_{\theta 2} \rangle$, the function

$$g(\phi) = \frac{v_z(b_2,\phi)}{v_\theta(b_2,\phi) - k b_2 v_z(b_2,\phi)},$$

$$= \frac{v_{z,h}(b_2,\phi) + U_0}{v_{\theta,h}(b_2,\phi) - k b_2 (v_{z,h}(b_2,\phi) + U_0)} \tag{18}$$

is considered a ''distribution function'' and $v_{\theta,h}, v_{z,h}$ are the components of the vector $\mathbf{v}_h$ defined in Eq. (9).

C. Summarized constraint equations

The equations

$$\Gamma = \Gamma_0 ,$$

$$\pi b_2^2 U_0 = \pi b_1^2 U_1 - \oint_C \mathbf{A}_h(r,\phi,R,\lambda,\Gamma).d\mathbf{l},$$

$$b_1 v_{\theta 1} = b_2 \frac{\int_0^{2\pi} g(\phi) v_{\theta 2}(\phi) d\phi}{\int_0^{2\pi} g(\phi) d\phi} \tag{19}$$

are a set of conditions which must be satisfied by the helical vortex flow in the downstream region. They constitute a nonlinear algebraic equations system for the variable parameters Γ, U_0, λ and R. The first and second conditions (19) immediately give the Γ value and the function $U_0(R,\lambda)$, which in turn gives the value of U_0 as a function of R and λ. Moreover, the last condition (19) is an undetermined nonlinear equation for the other two variable parameters, λ and R, of the helical flow. For a given value of λ, the equation becomes determined. In this way, solving numerically this equation for each value of λ (by bisection, evaluating the integrals for each value of the parameters), we obtain the possible values for R. (For a given λ, we can obtain two, one or none values of R, as we see in Fig. 6.)

The curves in Fig. 6 show the values of R as a function of λ obtained by solving the last equation (19) for different values of the swirl ratio $\Omega = \Gamma_0 b_2/2\pi Q$, where $Q = \pi b_1^2 U_1$ is the flow rate. In the following, we do not consider the trivial case $R=0$. [Notice that in this case the flow is axially symmetric (these conditions are always satisfied for the trivial solution, corresponding to an axisymmetric flow, $R=0$, $v_\theta = \Gamma/2\pi r$, $v_z = (b_1^2/b_2^2)U_1$. However, this solution is not interesting here, because it is not a helical flow.]

It is remarkable that the solutions (in λ) of Eq. (19) always have the opposite sign than Ω. This means that the geometrical sense of the helical filament is the opposite of the rotation sense of the upstream vortex. This result agrees with the experimental observations reported by Sarpkaya[10] and cited by Leibovich.[11]

Moreover, the curves of Fig. 6 show that the solutions (in λ) of Eq. (19), have a module $|\lambda|$ confined to a range between $(0,|\lambda|_{\max})$. The upper bound $|\lambda|_{\max}$ depends strongly on Ω. Figure 7 shows the contour plot of $|\lambda|_{\max}$ as function of Ω and b_2/b_1. Furthermore, from the curve of Fig. 6 for $\Omega = 0.16$, the solutions of the lower branch with $|\lambda| < 6$ have a very small R. If we are interested in considering only helical flows of significant amplitude, then the range of permissible $|\lambda|$ can be reduced. For example, in the case $\Omega = 0.16$, the $|\lambda|$ values are actually in the range (1, 4.4). In the next section, we consider some consequences and applications of these results.

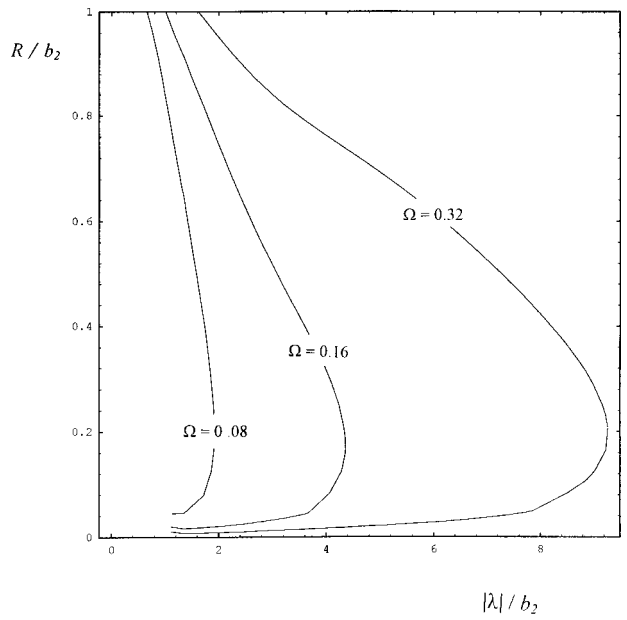

FIG. 6. Solutions curves of Eqs. (18). The points on the curves represent the admissible values of the parameters pair (R,λ) of a helical vortex flow developed downstream, for the values of the swirl ratio Ω showed on the curves.

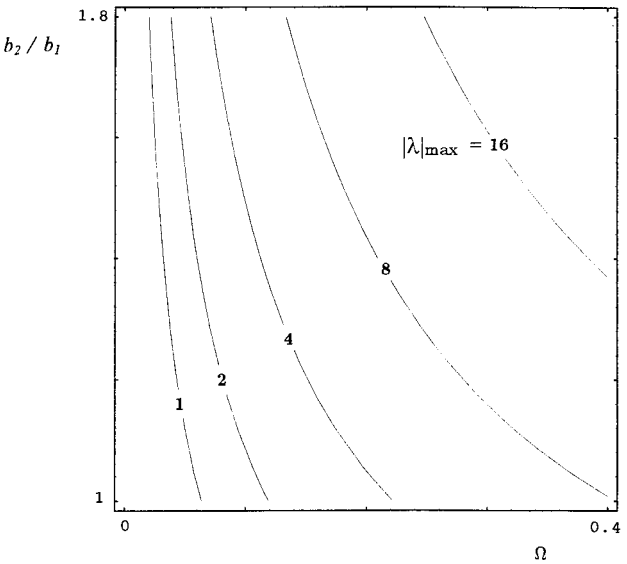

FIG. 7. Maximum allowed value of the pitch $\lambda_{\max}$ in function of the ratio b_2/b_1 and the swirl parameter Ω.

V. VORTEX STABILITY

A review of vortex stability is given by Leibovich.[11] At the present moment, a general criterion for the stability, to helical perturbations, of vortex flows in an inviscid incompressible fluid, is unknown. However, particular criteria are obtained for several simple cases. Thus Howard and Gupta[12] found a sufficient condition for the stability of an axial symmetric flow between concentric cylinders with axial velocity component $v_z(r)$ and swirl component $v_\theta(r)$, to axisymmetric disturbances. This condition is

$$\Phi-\frac{1}{4}\left(\frac{dv_z}{dr}\right)^2\geqslant 0, \tag{20}$$

where $\Phi=r^{-3}(d/dr)(r^2v_\theta^2)$. These authors also showed, for helical perturbations of the form

$$\{\delta v_r,\delta v_\theta,\delta v_z\}=\{f(r),g(r),h(r)\}\exp[in\theta+ik(z-ct)], \tag{21}$$

that the flow is stable when the condition

$$k^2\Phi-(2kn/r^2)v_\theta\frac{dv_z}{dr}-\frac{1}{4}\left[\left(k\frac{dv_z}{dr}+n\frac{d}{dr}(v_\theta/r)\right]^2\geqslant 0\right. \tag{22}$$

is satisfied everywhere inside the fluid. This condition is always violated for sufficiently small values of $|k|$, so no general stability criterion is obtained in this way. However, this condition permits us to determine a range of values of k corresponding to stable waves. We note that the perturbation (21) corresponds to a helix with pitch $\lambda=2\pi/k$.

On the other hand, in some cases it is possible, making a normal mode analysis, to obtain the dispersion relation, and then to determine the flow stability. For example, Lessen *et al.*[13] have studied in this way the linear stability of the unbounded rotating top-hat jet. In this paper we are concerned with bounded flows, thus we now briefly study the linear stability of this flow bounded by a cylindrical surface $r=b$, with velocity components

$$\begin{aligned} &v_z=U_1,\ v_\theta=\Omega r,\ v_r=0,\quad 0\leqslant r\leqslant a,\\ &v_z=0,\ v_\theta=a^2\Omega/r,\ v_r=0,\quad a\leqslant r\leqslant b. \end{aligned} \tag{23}$$

If we assume that the disturbances are of the form

$$\begin{aligned} &\{\delta v_r,\delta v_\theta,\delta v_z,\delta p\}\\ &=\{f(r),g(r),h(r),\pi(r)\}\exp[in\theta+ik(z-ct)], \end{aligned} \tag{24}$$

the linearized disturbance equations for an inviscid fluid with velocity profile (23) are

$$\begin{aligned} &\frac{1}{r}\frac{d}{dr}(rf)+in\frac{g}{r}+ikh=0,\\ &if\left(\frac{v_\theta}{r}n+(v_z-c)k\right)-2g\frac{v_\theta}{r}=-\frac{d}{dr}\pi,\\ &ig\left(\frac{v_\theta}{r}n+(v_z-c)k\right)+f\left(\frac{dv_\theta}{dr}+\frac{v_\theta}{r}\right)=-in\frac{\pi}{r},\\ &ih\left(\frac{v_\theta}{r}n+(v_z-c)k\right)=-ik\pi. \end{aligned} \tag{25}$$

After eliminating the other variables, we get, in each region, a Bessel equation for the z-component of the disturbance, h. Solving this equation, we obtain an expression for h (in both regions),

$$\begin{aligned} &h=C_1I_n(\mu r)+D_1K_n(\mu r),\quad 0\leqslant r\leqslant a,\\ &h=C_2I_n(kr)+D_2K_n(kr),\quad a\leqslant r\leqslant b, \end{aligned}$$

where $\mu^2=k^2\{1-4\Omega^2/(\Omega n+(U_1-c)k)\}$. By requiring the solution to be bounded at $r=0$, we obtain that $D_1=0$. Moreover, from Eq. (25) we also obtained expressions for the other components of the disturbances,

$$\begin{aligned} &0\leqslant r\leqslant a\\ &f=-\frac{ikC_1}{\mu^2}\left[\frac{2n\Omega}{r(n\Omega+(U_1-c)k)}I_n(\mu r)+\mu I_n'(\mu r)\right],\\ &\pi=-\alpha^{-1}[n\Omega+(U_1-c)k]C_1I_n(\mu r); \end{aligned} \tag{26}$$

$$\begin{aligned} &a\leqslant r\leqslant b\\ &f=-iC_2I_n'(kr)-iD_2K_n'(kr),\\ &\pi=-k^{-1}[na^2\Omega/r^2-ck](C_2I_n(\mu r)+D_2K_n(\mu r)). \end{aligned} \tag{27}$$

Boundary condition (5) implies that $f(b)=0$, and then

$$D_2=-[I_n'(kb)/K_n'(kb)]C_2. \tag{28}$$

Now, we suppose that the radial displacement of the vortex sheet due to the disturbance is $\Delta=A\exp(in\theta+ik(z-ct))$. The fact that the surface $r=a+\Delta$ moves with the fluid gives the kinematical condition

$$\frac{D\Delta}{Dt}\equiv\frac{\partial\Delta}{\partial t}+(\mathbf{U}\cdot\boldsymbol{\nabla})\boldsymbol{\Delta}=\delta v_r, \tag{29}$$

which must be satisfied in both sides of the surface, being $\mathbf{U}=(v_r,v_\theta,v_z)$ the unperturbed velocity.

The dynamical condition on the pressure states that it must be continuous across the surface $r=a+\Delta$ and gives, after linearizing,

$$\left.\frac{dP_{0,1}}{dr}\right|_{r=a}\Delta+\pi_1(a)=\left.\frac{dP_{0,2}}{dr}\right|_{r=a}\Delta+\pi_2(a), \tag{30}$$

where the suffixes 1, 2 denote the inner and outer regions, respectively, and P_0 is the pressure of the unperturbed state. Equations (28), (30), (29), together with (26), (27), determine the dispersion relation

$$\frac{k}{\mu^2}\left[\frac{2n\Omega}{(n\Omega+(U_1-c)k)}+\mu\frac{I'(\mu a)}{I(\mu a)}\right]\left[(n\Omega-kc)^2\frac{H_n(ka)}{H_n'(ka)}\right]$$

$$-k^{-1}[n\Omega+(U_1-c)k]^2=0 \tag{31}$$

where, by definition, $H_n(kr)\equiv I_n(kr)-[I_n'(kb)/K_n'(kb)]K_n(kr)$.

As b/a tends to infinity, this equation approaches the one obtained by Lessen *et al.*[13] Solving Eq. (31) we can obtain the value of the complex phase velocity $c=c_r+ic_i$, and so determine the stability of the basic flow Eq. (23). When the imaginary part of the phase velocity c_i is positive, the flow is unstable. We have solved the dispersion relation (31) numerically. The values of c_i/U_1 as a function of ka are shown in Fig. 8 for the quotient value $b/a=10$. It is remarkable that the values of c_i are very close to those obtained by Lessen *et al.*, in the limit of infinite b. This result means that the boundary has small influence on the linear stability of the vortex, when the core size is small in relation with the material frontier radius. Only for values of a of the same order of b, do we obtain a significant difference between the values of the phase velocity for the bounded and the unbounded vortex.

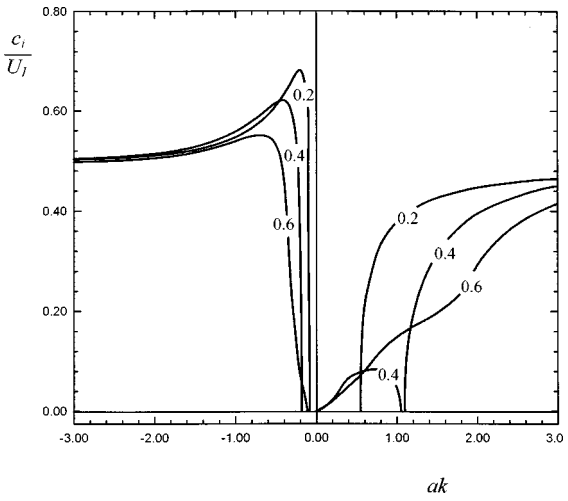

FIG. 8. Imaginary part of the velocity c_i for the disturbance to a rotating and confined top-hat jet, for $n=1$, $a/b=10$, and different values of Γ/aU_1 shown on the curves.

VI. APPLICATIONS OF NONLINEAR ANALYSIS OF ALLOWED FLOWS

Of course, the linear analysis is not valid when the helical flow has a large (finite) departure from an axially symmetric flow. In this case, the nonlinear analysis of allowed flows can be useful as a complement to the linear stability analysis. Knowledge of the range of allowed values of λ, for the full developed helical flow, can be used to check if a linear unstable mode can actually grow and develop into a helical flow. In order to clarify this point, let us study two concrete examples.

A. Example 1

First, we consider again, as in the previous section, the development of helical flows departing from the columnar vortex Eq. (23). The results of the linear analysis, for $U_1\neq 0$, are showed in Fig. 8. We see that, for helical perturbations (21) with wave number modulus $|k|=2\pi/|\lambda|$ sufficiently large, the flow is linearly unstable. In particular, when $\Gamma^*=\Gamma/aU_1=0.6$, the flow is unstable for all positive values of k, i.e., of the pitch λ. However, nonlinear analysis shows that the λ of waves with finite amplitude are contained in a range $(-|\lambda|_{\max},0)$, and then the unstable modes with $\lambda>0$ or with $\lambda<-|\lambda|_{\max}$ are not able to grow and develop helical flows. Of course, in these cases the instabilities can lead to another type of change in the flow, but not to helical flows. In particular, the inexistence of helical waves with $\lambda>0$ is in agreement with the experiments.[10,11] It is not possible to obtain this result from the linear analysis.[14,15]

B. Example 2

Now we consider the basic flow (in appropriate units)

$$u_z=V_0+\gamma AJ_0(\gamma r),\quad v_\theta=\frac{\gamma}{2}r+\gamma AJ_1(\gamma r),$$

$$v_r=0 \quad \text{for } 0\leqslant r\leqslant a;$$

$$v_z=1,\ v_\theta=\Gamma/r,\ v_r=0 \quad \text{for } a\leqslant r\leqslant b, \tag{32}$$

inside a tube of radius b, with continuity in the velocity [$J_0(x)$,$J_1(x)$ are the Bessel functions]. For the values $A=-0.04$, $a=0.2$, $b=1$, $\gamma=6$ the linear criterion (22) guarantees stability under perturbations (21) with λ in the range $(-54, 1.04)$. The system can be unstable under perturbations with λ out of this interval, which violate the criterion. For these values of the parameters, the swirl ratio $\Omega=0.038$. Nonlinear analysis of Sec. IV implies (for $b=1$, $\Omega=0.038$) that all possible helical flows have λ included in the interval $(-0.62, 0)$. We note that the pitch of the waves which violates the stability criterion is out of this last range. Then, no helical flow will develop departing from the basic flow Eq. (32) for the given values of the parameters. On the other hand, when $\gamma=20$, with the same values of a and b, the range of λ which satisfies the stability condition (22) is $(-1.35, 0.026)$, which does not contain the allowed interval $(-2.54, 0)$ obtained from our nonlinear analysis. Therefore, in this case, there are unstable modes which can develop helical flows.

VII. CONCLUSIONS

In this paper a study of the allowed helical flows inside a circular tube is presented. The flow is supposed irrotational except in a core of infinitesimal section. An expression for the flow around this helical filament is obtained. The boundary conditions are satisfied, calculating numerically the image for the helical vortex. Conservation laws are imposed to the helical flow, supposing a given upstream flow. Using this procedure, a dependence between pitch λ and amplitude R of

the helix is obtained. A range for admissible λ, for helical vortex flows with finite amplitude developed from an axially symmetric basic flow, is also found. The results are independent of the cutoff distance d, which is a fortunate fact, because the determination of d constitutes a serious problem.[4,8] Experimental observations (sense of the helix) are explained by this theory. The present analysis, which considers the effects of nonlinear terms in the balancing of conserved quantities, may be used to complement linear studies of stability, as it was shown before in two simple examples.

ACKNOWLEDGMENTS

This work was supported in part by the Programa de Desarrollo de las Ciencias Básicas (PEDECIBA, Uruguay) and by a project CONICYT–Clemente Estable of the Consejo Nacional de Investigaciones Científicas Y Técnicas (CONICYT, Uruguay). We would like to thank Dr. R. Guarga for bringing this problem to our attention and for helpful comments and suggestions.

[1] J. Faler and S. Leibovich, ''Disrupted states of vortex flow and vortex breakdown,'' Phys. Fluids **20**, 1385 (1977).
[2] A. K. Garg and S. Leibovich, ''Spectral characteristics of vortex breakdown flow fields,'' Phys. Fluids **22**, 2053 (1979).
[3] J. Harvey, ''Some observations of the vortex breakdown phenomena,'' J. Fluid Mech. **14**, 589 (1962).
[4] G. K. Batchelor, *An Introduction to Fluids Dynamics* (Cambridge, University Press, Cambridge, 1967).
[5] T. S. Lundgren and W. T. Ashurst, ''Area-varying waves on curved vortex tubes with application to vortex breakdown,'' J. Fluid Mech. **200**, 283 (1989).
[6] J. S. Marshall, ''A general theory of curved vortices with circular cross-section and variable core area,'' J. Fluid Mech. **229**, 311 (1991).
[7] Z. Rusak and A. Seginer, ''Propagation of small-amplitude displacement waves on a vortex in the center of a circular tube,'' Phys. Fluids A **5**, 578 (1993).
[8] S. E. Widnall, ''The structure and dynamics of vortex filaments,'' Annu. Rev. Fluid Mech. **7**, 141 (1975).
[9] L. M. Milne-Thomson, *Theoretical Hydrodynamics* (Macmillan, New York, 1949).
[10] T. Sarpkaya, ''Vortex breakdown in swirling conical flows,'' AIAA J. **8**, 1792 (1971).
[11] S. Leibovich, ''Vortex stability and breakdown: Survey and extension,'' AIAA J. **22**, 1192 (1983).
[12] L. N. Howard and A. S. Gupta, ''On the hydrodinamics and hydromagnetic stability of swirling flows,'' J. Fluid Mech. **14**, 463 (1962).
[13] M. Lessen, V. N. Deshpande, and B. Hadji-Ohanes, ''Stability of a potential with a non-rotating and rigid-body rotating top-hat jet core,'' J. Fluid Mech. **60**, 459 (1973).
[14] M. Lessen, P. J. Singh, and F. Paillet, ''The stability of a trailing line vortex. Part 1. Inviscid theory,'' J. Fluid Mech. **63**, 753 (1974).
[15] E. W. Mayer and K. G. Powell, ''Viscous and inviscid instabilities of a trailing vortex,'' J. Fluid Mech. **245**, 91 (1992).